ADAM-SINDy: An Efficient Optimization Framework for Parameterized Nonlinear Dynamical System Identification

Siva Viknesh[a,b], Younes Tatari[a,b], Amirhossein Arzani[a,b,*]

[a]*Department of Mechanical Engineering, University of Utah, Salt Lake City, UT, USA*
[b]*Scientific Computing and Imaging Institute, University of Utah, Salt Lake City, UT, USA*

Abstract

Identifying nonlinear dynamical systems characterized by nonlinear parameters presents significant challenges in deriving mathematical models that enhance understanding of physical phenomena. Traditional methods, such as Sparse Identification of Nonlinear Dynamics (SINDy) and symbolic regression, can extract governing equations from observational data; however, they also come with distinct advantages and disadvantages. This paper introduces a novel methodology within the SINDy framework, termed ADAM-SINDy, which synthesizes the strengths of established approaches by employing the ADAM optimization algorithm. This integration facilitates the simultaneous optimization of nonlinear parameters and coefficients associated with nonlinear candidate functions, enabling efficient and precise parameter estimation without requiring prior knowledge of nonlinear characteristics such as trigonometric frequencies, exponential bandwidths, or polynomial exponents, thereby addressing a key limitation of the classical SINDy framework. Through an integrated global optimization, ADAM-SINDy dynamically adjusts all unknown variables in response to system-specific data, resulting in a more adaptive and efficient identification procedure that reduces the sensitivity to the library of candidate functions. The performance of the ADAM-SINDy methodology is demonstrated across a spectrum of dynamical systems, including benchmark coupled nonlinear ordinary differential equations such as oscillators, chaotic fluid flows, reaction kinetics, pharmacokinetics, as well as nonlinear partial differential equations (wildfire transport). The results demonstrate significant improvements in identifying parameterized dynamical systems and underscore the importance of concurrently optimizing all parameters, particularly those characterized by nonlinear parameters. These findings highlight the potential of ADAM-SINDy to extend the applicability of the SINDy framework in addressing more complex challenges in dynamical system identification.

Keywords: Sparse regression; Model discovery; Nonlinear dynamical systems; Interpretable machine learning

1. Introduction

System identification is a crucial aspect of accurately modeling the dynamics of physical, chemical, and biological systems. By providing a mathematical representation of these systems, system identification enables essential predictions, interpretation, optimization, and control strategies across diverse applications, from engineering to environmental science [1]. The process typically involves determining a system's mathematical model from observed data, using methods such as

---

*Corresponding author
Email address:* `amir.arzani@sci.utah.edu` (Amirhossein Arzani)

least squares, subspace identification, or frequency domain analysis. The process includes data collection, model structure selection, parameter estimation, validation, and refinement.

Machine learning significantly enhances system identification by offering advanced tools for modeling complex, nonlinear systems and uncovering hidden patterns in data. Techniques such as supervised learning, neural networks, reinforcement learning, and Gaussian processes facilitate flexible, data-driven modeling. The integration of machine learning with traditional system identification has led to the development of methodologies for linear [2], nonlinear [3], hybrid [4], and parametric/non-parametric [5] dynamical systems. Although linear models are often simpler and computationally efficient, practical systems frequently contain nonlinear features that necessitate more sophisticated models. Addressing the challenge of defining appropriate models for nonlinear systems often requires expert insight. Despite significant progress in earlier research [6, 7], nonlinear system identification remains a vibrant and promising research area. The increasing availability of data and advancements in computational methods have led to the development of automated techniques for nonlinear system identification. Recent advancements include methods such as genetic algorithms [8], symbolic regression [9], and deep learning-based algorithms [10, 11, 12, 13, 14], which have proven effective in deriving governing nonlinear equations from empirical data. These methods aim to generate meaningful models from data with minimal reliance on prior assumptions, making them particularly valuable when traditional model hypotheses are unavailable.

An important aspect of data-driven system identification is the interpretability of the identified system, which is often accomplished through the use of a limited number of terms in an analytical equation. This characteristic not only establishes a meaningful connection between system identification studies and explainable artificial intelligence (XAI) but also underscores the significance of transparency in modeling complex phenomena. In the realm of XAI, interpretable models are developed to explain the decisions of opaque neural networks (post-hoc XAI) or to enhance interpretability from the construction phase of the machine learning architecture (by-design XAI) [15, 16, 17]. Importantly, the system identification methods presented in this study exemplify the principles of by-design XAI.

Symbolic regression provides a unique and interpretable method for system identification, blending classical equation-based approaches with advanced optimization techniques to produce insightful models [18]. Currently, the use of genetic algorithms represents the state-of-the-art in symbolic regression [19, 20]. These algorithms effectively mimic natural selection by evolving a population of candidate models over successive generations. Through essential operations such as crossover, mutation, and selection, genetic algorithms efficiently search for equations that optimally capture the system dynamics. This comprehensive process not only facilitates the simultaneous discovery of both the structure and parameters of governing equations but also proves particularly effective in capturing intricate system behaviors. However, it is often susceptible to the bloating effect [21], where candidate solutions become overly complex, hindering interpretability and reducing the generalizability of the identified models. Despite its strengths, symbolic regression faces challenges in capturing chaotic systems due to difficulties in effective phase space sampling, often mitigated through embedding methods [22, 23]. Recent advancements, such as diffusion maps [24, 25] and local linear embedding [26], address the curse of dimensionality by operating directly on the manifold of the dynamical system, improving the ability to capture complex behaviors. Moreover, innovations like linear basis initialization [27, 28], fast function extraction [9], gradient-based optimization [29], invoking system symmetries/manifolds [30], and physics-constrained optimization [31] have significantly enhanced the performance of symbolic regression in predicting and identifying dynamical systems.

As an alternative to symbolic regression, sparsity-promoting techniques that represent nonlinear

equations as a sparse combination of basis functions from a comprehensive dictionary have been proposed, offering a computationally efficient alternative [32, 33]. The Sparse Identification of Nonlinear Dynamics (SINDy) framework [34] is a widely recognized methodology for discovering interpretable and parsimonious mathematical models that balance accuracy and simplicity. It is based on the principle that many physical dynamical systems can be described by parsimonious models, where only a small set of terms is needed to represent the system's dynamics. By framing the identification problem as a sparse regression problem, SINDy facilitates the discovery of compact, interpretable models while avoiding the computational intensity associated with symbolic regression. This sparsity-driven approach mitigates the risk of overfitting and simplifies the model selection process.

Unlike the broad unstructured search employed in symbolic regression, SINDy operates within a constrained framework where candidate functions are drawn from a predefined library of candidate terms. This structured approach significantly reduces the computational burden. It allows for a more targeted and controlled exploration of the governing equations, ensuring that only the most relevant terms are retained in the final model. This methodology not only enhances computational efficiency but can also improve interpretability. Furthermore, SINDy has demonstrated its effectiveness across various domains, including fluid dynamics [35], plasma dynamics [36], turbulence closures [37], chaotic systems [38], and computational chemistry [39]. Additionally, SINDy has been extended to applications such as nonlinear model predictive control [40], rational functions [41, 42], enforcing conservation laws and symmetries [35], interpretable operator learning [43], promoting stability [44], and generalizing for stochastic dynamics [45], including Bayesian perspectives [46].

Comparing symbolic regression and the SINDy methodologies for the identification of dynamical systems reveals several key differences that impact their application and efficiency. Symbolic regression does not necessitate prior knowledge of parameters associated with the complex behavior of a system, such as Fourier frequencies and exponential growth/decay rates. Instead, it searches through a vast space of mathematical operators and nonlinear functions, such as polynomials, trigonometrics, and logarithms, to construct an equation that best fits the given data. However, this exploratory nature of symbolic regression often entails considerable computational demands, necessitating extensive computational resources. Moreover, it may yield varying results for identical datasets and hyperparameters, posing challenges for reproducibility. In contrast, the SINDy framework *does* require prior knowledge of nonlinear parameters such as frequencies to effectively guide the optimization process. Without such preliminary information, SINDy may struggle to yield an accurate mathematical model, potentially leading to sub-optimal performance. Nevertheless, when the necessary parameters are known or when a distribution of parameter ranges is considered that contains the correct parameter, SINDy offers a considerable computational advantage. It can derive the desired mathematical model in a fraction of the computational time required by symbolic regression. This efficiency is attributed to its formulation of the identification problem as a sparse regression task and a convex optimization problem, which streamlines the model selection process and reduces computational overhead.

While both symbolic regression and SINDy offer distinct advantages and limitations, their comparative strengths highlight the importance of continued advancements in nonlinear system identification. In this work, we adopted an optimization algorithm leveraging Stochastic Gradient Descent–ADAM optimization, implemented using the PyTorch machine learning framework, to significantly improve the classical SINDy methodology. This augmented approach, termed ADAM-SINDy, integrates key advantages of symbolic regression, such as the simultaneous optimization of nonlinear parameters (e.g., frequencies and exponential growth/decay rates), alongside the selection of the most appropriate candidates from a comprehensive library of functions. Its effectiveness

stems from leveraging the computational graph of the gradient descent algorithm for efficient back-propagation and dynamic interactions between all the trainable parameters, thus enhancing the robustness and precision of system identification, particularly in complex dynamical systems where the traditional SINDy method struggles. It is important to note that while ADAM-SINDy is not designed to surpass symbolic regression in all aspects, its primary goal is to address the limitations of the classical SINDy framework, particularly in nonlinear parameter estimation. By enhancing SINDy's capability to simultaneously identify nonlinear parameters and select candidate functions, ADAM-SINDy offers a more efficient and scalable approach to identifying parameterized dynamical systems. This improvement broadens the applicability of the SINDy framework, making it more effective for complex and high-dimensional systems.

Our present work makes several key contributions:

- The SINDy framework is augmented with ADAM optimization, termed ADAM-SINDy, which enables the simultaneous estimation of nonlinear parameters while identifying parsimonious and relevant candidate terms. This enhancement addresses a significant limitation of the classical SINDy method, which traditionally requires exact knowledge of the parameters in its library of candidate terms.

- The ADAM-SINDy framework integrates concurrent hyperparameter optimization (the sparsity knob) during the identification process, thereby mitigating the need for extensive manual tuning. In contrast, the classical SINDy approach, although capable of producing parsimonious models, is sensitive to the sparsity knob value, necessitating a delicate balance between accuracy and model complexity.

- ADAM-SINDy introduces a candidate-wise sparsity knob, resulting in a "fully" adaptive LASSO methodology. This innovative approach selectively penalizes incorrect terms while retaining the relevant ones throughout the optimization process, employing a concurrent, adaptive individual weighting strategy that is absent in the classical SINDy method.

- Through the integration of a global optimization strategy, the ADAM-SINDy framework allows self-adaptation of nonlinear functions and interaction between candidate terms. This adaptability is crucial when predefined candidates are lacking, as it optimizes parameters to compensate for missing functions. In contrast, the classical SINDy approach is limited by static parameters and the absence of interaction, increasing the risk of incorrect system models when essential candidate functions are missing.

- The novel ADAM-SINDy optimization methodology allows for the incorporation of differential operator-based loss functions, akin to high-order Tikhonov regularization. This methodology provides an environment that can directly incorporate governing differential equations into the optimization process, thereby accelerating loss decay and improving convergence rates.

The paper is structured as follows. Section 2 provides an overview of the classical SINDy methodology, outlining its mathematical foundation and then introducing the ADAM-SINDy methodology, emphasizing its advantages and the implementation of the gradient descent algorithm. This section also details the master candidate library of nonlinear functions used in evaluating the classical SINDy and ADAM-SINDy frameworks. Section 3 examines benchmark problems across various applications, including ordinary and partial differential equations, focusing on problems that have nonlinear parameters, thereby challenging the classical SINDy method. Section 4 discusses the advantages of the ADAM-SINDy method over the classical approach. Finally, Section 5 presents a conclusion.

2. Methods

2.1. Sparse Identification of Nonlinear Dynamics (SINDy)

The SINDy algorithm is an efficient nonlinear system identification approach, grounded in the principle that the governing equations of a nonlinear system can be effectively represented by a sparse combination of appropriate pre-defined candidate basis functions [34]. The central objective of SINDy is to identify a minimal set of relevant basis functions from an extensive dictionary of candidate functions, leveraging sparsity–promoting techniques to achieve an optimal balance between model complexity and accuracy.

Consider the problem of identifying nonlinear dynamical systems described by the differential equation

$$\dot{\mathbf{x}}(t) = \mathbf{f}(\mathbf{x}(t)) , \tag{1}$$

where $\mathbf{x}(t) \in \mathbb{R}^n$ denotes the state vector at time t, $\dot{\mathbf{x}}(t)$ represents its time derivative, and $\mathbf{f}(\mathbf{x})$: $\mathbb{R}^n \to \mathbb{R}^n$ is a nonlinear function governing the system's dynamics. The objective of the SINDy algorithm is to identify the function $\mathbf{f}(\mathbf{x}(t))$ from available data. The process begins by collecting a dataset consisting of measurements of m states at n discrete time-steps. The data is organized as follows:

$$\mathbf{X} = \begin{bmatrix} \mathbf{x}(t_1)^\top \\ \mathbf{x}(t_2)^\top \\ \vdots \\ \mathbf{x}(t_n)^\top \end{bmatrix} = \begin{bmatrix} \mathbf{x}_1(t_1) & \mathbf{x}_2(t_1) & \cdots & \mathbf{x}_m(t_1) \\ \mathbf{x}_1(t_2) & \mathbf{x}_2(t_2) & \cdots & \mathbf{x}_m(t_2) \\ \vdots & \vdots & \ddots & \vdots \\ \mathbf{x}_1(t_n) & \mathbf{x}_2(t_n) & \cdots & \mathbf{x}_m(t_n) \end{bmatrix} , \tag{2}$$

where each row represents a snapshot of the states at a given time. The matrix $\mathbf{X} \in \mathbb{R}^{n \times m}$ contains the state vectors $\mathbf{x}(t_i)$, each corresponding to the system's state at time t_i. Similarly, the time derivatives of the state vectors, denoted as $\dot{\mathbf{X}} \in \mathbb{R}^{n \times m}$, are represented as follows:

$$\dot{\mathbf{X}} = \begin{bmatrix} \dot{\mathbf{x}}(t_1)^\top \\ \dot{\mathbf{x}}(t_2)^\top \\ \vdots \\ \dot{\mathbf{x}}(t_n)^\top \end{bmatrix} = \begin{bmatrix} \dot{\mathbf{x}}_1(t_1) & \dot{\mathbf{x}}_2(t_1) & \cdots & \dot{\mathbf{x}}_m(t_1) \\ \dot{\mathbf{x}}_1(t_2) & \dot{\mathbf{x}}_2(t_2) & \cdots & \dot{\mathbf{x}}_m(t_2) \\ \vdots & \vdots & \ddots & \vdots \\ \dot{\mathbf{x}}_1(t_n) & \dot{\mathbf{x}}_2(t_n) & \cdots & \dot{\mathbf{x}}_m(t_n) \end{bmatrix} . \tag{3}$$

This dataset is utilized as input to the system identification problem. A library of candidate functions, denoted $\boldsymbol{\Theta}(\mathbf{X}, \boldsymbol{\Lambda}) \in \mathbb{R}^{n \times p}$, is constructed, encompassing p number of functions, such as polynomials and trigonometric functions. A typical representative library is given below

$$\boldsymbol{\Theta}(\mathbf{X}; \boldsymbol{\Lambda}) = \begin{bmatrix} 1 & \mathbf{X}^{\mathcal{A}} & \dots & \sin(\mathcal{B}\mathbf{X}) & \dots & \mathbf{X} \otimes \exp(\mathcal{C}\mathbf{X}) \end{bmatrix} , \tag{4}$$

where each column of $\boldsymbol{\Theta}(\mathbf{X}; \boldsymbol{\Lambda})$ represents a candidate function derived from the state vector $\mathbf{X}$ for the given nonlinear parameters $\boldsymbol{\Lambda} \in \{\mathcal{A}, \mathcal{B}, \mathcal{C}\}$, which correspond to the highest polynomial order, Fourier frequencies, and exponential exponents, respectively, typically chosen to define the extensive candidate library. These nonlinear parameters must be either predetermined prior to the optimization process, which is often impractical in real-world engineering problems, or defined within a specified distribution range, which can result in an extensive candidate matrix and risk missing the precise parameter. Accurate determination of these parameters is a crucial step for constructing the candidate functions and effectively identifying the most relevant functions for characterizing the system's dynamics.

The goal in SINDy is to select a subset of these candidate functions, which is achieved by formulating a sparse regression problem and aiming to determine a sparse corresponding coefficient vector $\boldsymbol{\Xi} = [\boldsymbol{\xi}_1, \boldsymbol{\xi}_2, \ldots, \boldsymbol{\xi}_m] \in \mathbb{R}^{p \times m}$ indicating the active features from the dictionary $\boldsymbol{\Theta}(\mathbf{X}; \boldsymbol{\Lambda})$, such that their weighted sum accurately describes $\mathbf{f}(\mathbf{x}(t))$. Mathematically, this is expressed as

$$\dot{\mathbf{X}} = \boldsymbol{\Theta}(\mathbf{X}; \boldsymbol{\Lambda})\,\boldsymbol{\Xi} \ . \tag{5}$$

Sparsity-promoting regularization methods, such as LASSO [47, 48], are commonly used to enforce sparsity in $\boldsymbol{\Xi}$, i.e., making most of its entries zero. However, LASSO does not always guarantee the sparsest solution, and alternative methods [49, 50] may require prior knowledge of the expected number of non-zero elements in $\boldsymbol{\Xi}$, which is often unknown. The LASSO augmented with a sequential thresholding approach [34], which iteratively solves least-squares problems and prunes coefficients below a given threshold, offers a more flexible alternative. The sparse regression problem can be formulated as

$$\min_{\boldsymbol{\Xi}} \left[\|\dot{\mathbf{X}} - \boldsymbol{\Theta}(\mathbf{X}; \boldsymbol{\Lambda})\,\boldsymbol{\Xi}\|_2^2 + \lambda \|\boldsymbol{\Gamma}\,\boldsymbol{\Xi}\|_1 \right] \ , \tag{6}$$

where λ is a regularization parameter that enforces sparsity in the solution, balancing model complexity with accuracy. In the classical SINDy methodology [34], $\boldsymbol{\Gamma} \in \mathbb{R}^{p \times p}$ is typically assumed to be an identity matrix. However, in more general settings where $\boldsymbol{\Gamma}$ is a non-identity matrix, it scales the individual candidate functions and remains fixed throughout the optimization process, as in the Adaptive LASSO [51]. Furthermore, if $\boldsymbol{\Gamma}$ represents a differential operator, such as a gradient or Laplacian, the regularization approach resembles higher-order Tikhonov regularization [52]. Upon solving, the SINDy identified dynamical model is expressed as:

$$\dot{\mathbf{x}}(t) = \boldsymbol{\Theta}(\mathbf{x}(t))\boldsymbol{\Xi} \ . \tag{7}$$

The SINDy approach provides a parsimonious and interpretable framework for uncovering the underlying dynamics of a system by exploiting sparsity within a known function basis. This methodology is particularly advantageous when the governing equations are not fully known but are presumed to be sparse within the space of candidate functions.

2.2. ADAM Optimization Augmented SINDy: ADAM-SINDy

The ADAM-SINDy methodology, a novel extension of the traditional SINDy framework [34], introduces substantial improvements by adopting ADAM optimization in place of the more commonly employed iterative least squares algorithm for solving the LASSO problem. This methodological innovation significantly addresses key challenges in parameter estimation, while concurrently reducing the dependency on the predefined library of candidate functions, a key limitation that has often constrained the SINDy approaches. Unlike the classical SINDy framework, which heavily relies on the initial selection of candidate parameters, ADAM-SINDy *adaptively* identifies relevant terms from the candidate library ($\boldsymbol{\Xi}$) while simultaneously optimizing nonlinear parameters ($\boldsymbol{\Lambda}$). This adaptive process minimizes reliance on prior assumptions and enhances the capability to discover complex, nonlinearly defined parameters in a more robust manner. Nonlinear parameters, such as frequencies in trigonometric functions, bandwidths in exponential functions (e.g., kernels), and non-integer polynomial exponents, present challenges in the traditional SINDy approach, which requires prior knowledge of these parameters. ADAM-SINDy addresses this limitation by making these parameters optimizable within a global optimization framework. The incorporation of stochastic gradient descent within the ADAM-SINDy framework yields several distinct improvements over the conventional SINDy approach:

1. **Simultaneous optimization:** ADAM-SINDy concurrently optimizes hyperparameters and identifies both nonlinear parameters and relevant candidate functions. Unlike SINDy, the proposed method does not require any prior knowledge about the nonlinear parameters in the candidate functions. ADAM-SINDy's integrated optimization framework reduces the need for extensive tuning processes, which are often required in traditional SINDy via trial-and-error methods or sequential optimization steps.

2. **Adaptive scaling:** ADAM-SINDy treats the regularization parameter, $\mathbf{\Gamma}$, as an optimizable matrix, transforming into a "fully" Adaptive LASSO. This approach facilitates the iterative scaling of each candidate function throughout the epoch iterations, offering a more flexible and adaptive weighting strategy compared to the conventional Adaptive LASSO, which lacks this level of dynamic adaptability. As a result, the method facilitates an individualized treatment of the candidate functions, thereby enhancing the accuracy of parameter identification and improving the overall robustness of the system identification process.

3. **Higher-order regularization:** Utilizing a computational graph, ADAM-SINDy further enables the opportunity to efficiently apply higher-order Tikhonov regularization, where the matrix $\mathbf{\Gamma}$ functions as a differential operator. This method is analogous to the physics-based loss functions used in Physics-Informed Neural Networks (PINN) [53], allowing for the imposition of complex constraints that ensure the identified model aligns closely with the governing physical laws. This augmented regularization framework guarantees that the identified dynamical system remains robust, interpretable, and consistent with the underlying physical principles. Here, we will briefly discuss this aspect and pursue the concept of physics-informed SINDy with ADAM-SINDy in future work.

The ADAM-SINDy framework, detailed in Algorithm 1, introduces a fully adaptive global optimization process for all parameters typically preselected in the classical SINDy framework. It begins with the initialization of key parameters—$\mathbf{\Xi}$, $\mathbf{\Lambda}$, λ, and $\mathbf{\Gamma}$—which are iteratively optimized based on the provided input data. To enhance computational efficiency and robustness, the input data is divided into batches of size B. When the batch size is set equal to the size of the input data, the algorithm operates under a full-batch optimization procedure. During each epoch, for each batch (or the full dataset in the case of full-batch optimization), the loss function $\mathcal{L}_b$ is computed to measure the discrepancy between the observed system dynamics, $\dot{\mathbf{X}}_b$, and the model's predicted dynamics, represented by $\mathbf{\Theta}(\mathbf{X}_b; \mathbf{\Lambda})\,\mathbf{\Xi}$. This batch-wise loss computation incorporates a sparsity-inducing term, regulated by λ and $\mathbf{\Gamma}$, ensuring that only the most relevant terms are selected.

The parameters—$\mathbf{\Xi}$, $\mathbf{\Lambda}$, λ, and $\mathbf{\Gamma}$—are then updated via the stochastic gradient descent algorithm on a per-batch basis, gradually minimizing the loss function across the entire dataset. In the case of full-batch optimization, updates are performed after computing the loss over the entire input dataset at once. A sequential thresholding step is employed after each batch update, where values of both $\mathbf{\Xi}$ and $\mathbf{\Lambda}$ that are small are set to zero if they fall below the specified tolerance, ϵ. This iterative process, which repeats for each batch and continues until the maximum number of iterations, N_{max}, is reached, ensures that the optimization converges efficiently.

2.2.1. Stochastic versus Full-Batch Optimization

The ADAM-SINDy framework provides the flexibility to implement both a batching strategy through stochastic gradient descent and a full-batch optimization approach. In the stochastic case, optimization is performed on smaller, randomly sampled subsets of the overall dataset. This

Algorithm 1 ADAM-SINDy Algorithm

Input:
  Observational data $\mathbf{X}$ and $\dot{\mathbf{X}}$
  Tolerance ϵ and maximum iterations $N_{\max}$
  Learning rate $\eta_{\boldsymbol{\Xi}}$, $\eta_{\boldsymbol{\Lambda}}$, η_{λ}, and $\eta_{\boldsymbol{\Gamma}}$
Initialization:
  Initialize $\boldsymbol{\Xi} \leftarrow \boldsymbol{\Xi}_0$, $\boldsymbol{\Lambda} \leftarrow \boldsymbol{\Lambda}_0$, $\lambda \leftarrow \lambda_0$, $\boldsymbol{\Gamma} \leftarrow \boldsymbol{\Gamma}_0$
  Set iteration counter $n \leftarrow 0$
Optimization Loop:
while $n < N_{\max}$ **do**
 For each batch $b = 1, 2, \ldots$
  Sample a batch of data $\mathbf{X}_b$ and $\dot{\mathbf{X}}_b$
  Compute $\boldsymbol{\Theta}(\mathbf{X}_b; \boldsymbol{\Lambda})$
  Compute Loss Function:

$$\mathcal{L}_b \leftarrow \left[\|\dot{\mathbf{X}}_b - \boldsymbol{\Theta}(\mathbf{X}_b; \boldsymbol{\Lambda})\,\boldsymbol{\Xi}\|_2^2 + \lambda\|\boldsymbol{\Gamma}\,\boldsymbol{\Xi}\|_1 \right]$$

  Update Parameters:
$$\boldsymbol{\Xi}_{n+1} \leftarrow \boldsymbol{\Xi}_n - \eta_{\boldsymbol{\Xi}}\,\nabla_{\boldsymbol{\Xi}}\,\mathcal{L}_b(\boldsymbol{\Theta}_b, \boldsymbol{\Xi}, \boldsymbol{\Lambda}, \lambda, \boldsymbol{\Gamma})$$

$$\boldsymbol{\Lambda}_{n+1} \leftarrow \boldsymbol{\Lambda}_n - \eta_{\boldsymbol{\Lambda}}\,\nabla_{\boldsymbol{\Lambda}}\,\mathcal{L}_b(\boldsymbol{\Theta}_b, \boldsymbol{\Xi}, \boldsymbol{\Lambda}, \lambda, \boldsymbol{\Gamma})$$

$$\lambda_{n+1} \leftarrow \lambda_n - \eta_{\lambda}\,\nabla_{\lambda}\,\mathcal{L}_b(\boldsymbol{\Theta}_b, \boldsymbol{\Xi}, \boldsymbol{\Lambda}, \lambda, \boldsymbol{\Gamma})$$

$$\boldsymbol{\Gamma}_{n+1} \leftarrow \boldsymbol{\Gamma}_n - \eta_{\boldsymbol{\Gamma}}\,\nabla_{\boldsymbol{\Gamma}}\,\mathcal{L}_b(\boldsymbol{\Theta}_b, \boldsymbol{\Xi}, \boldsymbol{\Lambda}, \lambda, \boldsymbol{\Gamma})$$

  Thresholding: For each element i, set $\boldsymbol{\Xi}_{n+1}^i, \boldsymbol{\Lambda}_{n+1}^i \leftarrow 0$ if $|\boldsymbol{\Xi}_{n+1}^i|, |\boldsymbol{\Lambda}_{n+1}^i| \leq \epsilon$
  Increment iteration counter: $n \leftarrow n + 1$
end while
Output:
  Optimized parameters $\boldsymbol{\Xi}^*$ and $\boldsymbol{\Lambda}^*$

method optimizes computational resource utilization by partitioning the data into manageable chunks, thereby reducing memory requirements and accelerating the optimization process. The batch size must be sufficiently large to capture the dynamics of interest while remaining small enough to facilitate efficient computation.

In contrast, full-batch optimization processes the entire dataset in a single iteration. This approach leverages all available information, potentially yielding more accurate and stable updates to the optimization parameters. Notably, ADAM optimization employs momentum, which can help avoid local minima even in the absence of stochasticity introduced by mini-batches.

While both methodologies share the same optimization strategy, a primary difference lies in the number of temporal data points considered in each optimization step. In the stochastic batching case, the batch size is typically smaller than the total number of available temporal data points. These data points are randomly sampled and shuffled, with the final batch potentially containing fewer points than the specified batch size. During implementation, temporal data is organized into rows based on the selected batch size, which dictates the number of rows in the ground truth data used in each optimization step. Then the candidate function matrix is constructed, reflecting the selected batch size through the number of rows it contains. Importantly, the dimensionality of the unknown nonlinear parameters and the coefficient matrix remains invariant, as the underlying dynamics of the system are independent of data partitioning based on time steps. Consequently, employing a batching strategy in the sparse regression problem enhances computational efficiency, reduces memory requirements, and facilitates effective manipulation of the matrix size.

2.3. Problem Statement

In this work, several benchmark dynamical systems problems are selected to illustrate the efficacy of the ADAM-SINDy framework and to underscore its advantages relative to the classical SINDy approach. All SINDy methodologies are built upon a common master library that incorporates a diverse range of nonlinear functions, including polynomials, Fourier terms, exponential functions, and nonlinear terms combined with polynomial expressions. This library is formally defined as follows:

$$\boldsymbol{\Theta} = \begin{bmatrix} 1 & \mathbf{X}^{\mathcal{A}} & \sin(\mathcal{B}\mathbf{X}) & \cos(\mathcal{C}\mathbf{X}) & \exp(\mathcal{D}\mathbf{X}) & \mathbf{X} \otimes \sin(\mathcal{E}\mathbf{X}) & \mathbf{X} \otimes \cos(\mathcal{F}\mathbf{X}) & \mathbf{X} \otimes \exp(\mathcal{G}\mathbf{X}) \end{bmatrix} , \quad (8)$$

where $\mathbf{X}$ denotes the input data, and $\mathcal{A}, \mathcal{B}, \mathcal{C}, \mathcal{D}, \mathcal{E}, \mathcal{F}, \mathcal{G}$ represent the adaptive nonlinear parameters ($\boldsymbol{\Lambda}$) that are subject to optimization within the ADAM-SINDy framework. Specifically, $\mathcal{A}$ is chosen to be 1, thereby encompassing polynomial terms up to the first order in the master library for all cases. However, in certain numerical experiments, $\mathcal{A}$ is rendered trainable when it corresponds to a non-integer rational exponent. It is noteworthy that the classical SINDy method relies on precise a priori knowledge of these parameters to successfully identify a sparse system.

The proposed ADAM-SINDy methodology also offers further significant advantages due to the trainable nature of the nonlinear parameters. Specifically, when the parameters associated with cosine and exponential functions—$\mathcal{C}$ and $\mathcal{D}$—approach zero, their non-zero coefficients effectively interact with the constant term 1 present in the library. Similarly, in the context of nonlinear polynomial combined terms, specifically those involving exponential and cosine functions, when $\mathcal{F}$ and $\mathcal{G}$ converge to zero, these terms interact with the polynomial terms $\mathbf{X}^{\mathcal{A}}$. This phenomenon of effective self-adaptation of nonlinear functions and its interaction with other functions, as distinctly observed in the ADAM-SINDy framework is particularly crucial in scenarios where predefined candidate functions lack an exact function required to accurately represent the true system dynamics, as the trainable parameters are optimized to compensate for these deficiencies.

In contrast, the classical SINDy method operates under the assumption of a convex loss landscape, where nonlinear parameters are generated by uniform sampling within a predefined range. This conventional approach not only restricts the flexibility of the parameters but also precludes interactions between candidate functions within the library, as evidenced in the ADAM-SINDy methodology. Consequently, the classical SINDy approach is inherently constrained by its reliance on static parameters, which significantly increases the likelihood of incorrect system identification, particularly when essential functions are absent from the candidate library. As a result, the classical SINDy method frequently struggles to accurately capture the true dynamics of the system, especially in scenarios with nonlinear parameters, wherein the rigidity of predefined parameters–coupled with the absence of precise values–further impedes the effective identification of governing equations.

To investigate these limitations, two variants of the classical SINDy approach are explored: the SINDy-W method and the SINDy-W/o method. The SINDy-W method represents a fortunate scenario (unlikely in practical complex problems) where the precise value of the unknown nonlinear parameter is included within the range of candidate parameters $\mathbf{\Lambda}$. While such a scenario may hold in controlled or well-defined environments, they are often inadequate in real-world engineering applications, where the underlying parameter values may be unknown or difficult to estimate. Conversely, the SINDy-W/o method assumes no prior knowledge of the parametric values and applies a broad range of distributed parameter values to account for a wider spectrum of possibilities. In our benchmark problems, the range of parameters is selected such that the unknown parameter falls within the range. The SINDy-W/o approach is the more realistic practical version of SINDy, however, it often struggles in cases when the predefined parameter ranges fail to contain the "exact value" required to capture the system's true behavior. This absence of prior knowledge frequently leads to less accurate, overly complex, and non-parsimonious models. Ultimately, these challenges underscore the need for flexibility and adaptability in parameter selection to ensure accurate system identification, motivating the use of the ADAM-SINDy framework, which dynamically adjusts parameter values during optimization and overcomes the limitations of the classical methods' predefined parameter spaces.

Here, we adopt the approach established in the classical SINDy method regarding the sparsity-promoting parameters λ and $\mathbf{\Gamma}$ [34]. Specifically, $\mathbf{\Gamma}$ is treated as a diagonal identity matrix, with the λ parameter being the sole variable used to control sparsity for the two variants considered: classical SINDy-W and SINDy-W/o methods. Notably, the numerical experiments conducted with the ADAM-SINDy framework indicate that the simultaneous optimization and utilization of both sparsity-promoting knobs is not essential; indeed, no significant differences in outcomes were observed when optimizing only one of these knobs.

The ADAM-SINDy methodology is implemented using the PyTorch library, considering both batch-wise and full-batch optimization strategies, and employs the ADAM optimizer to facilitate the simultaneous optimization of all unknown variables involved in the sparse regression problem, including the parameters $\mathbf{\Lambda}$, the coefficients $\mathbf{\Xi}$, and the sparsity knob $\mathbf{\Gamma}$, with the parameter λ fixed at a value of 1 and not subject to optimization. In this implementation, the parameter $\mathbf{\Lambda} \in \mathbb{R}^{m \times \hat{p}}$ is defined as a non-square scalar matrix associated with $\hat{p}$ nonlinear candidate parameters corresponding to each of the m state variables. This structure facilitates vectorization, allowing the ADAM optimizer to be invoked only once for all nonlinear parameters rather than for each individual value. Consequently, while $\mathbf{\Lambda}$ parameters behave like scalar values algorithmically, it is defined as a non-square scalar matrix for improved computational efficiency. Thus, the parameters $\mathbf{\Lambda}$ and $\mathbf{\Xi}$ are initialized as scalar matrices with all values of 1. Additionally, the diagonal matrix $\mathbf{\Gamma}$, with trainable diagonal entries, is initialized using a Gaussian distribution with a standard deviation of

1. To enhance convergence during the optimization process, a step decay variant for the dynamic learning rate is employed, systematically reducing the learning rate with a decay rate of 0.5 across all numerical experiments conducted in this research. Furthermore, during the sequential thresholding step, a tolerance value of 5×10^{-3} is utilized for ϵ, effectively eliminating small $\mathbf{\Xi}$ and $\mathbf{\Lambda}$ values. A comprehensive overview of the hyperparameters for both the classical SINDy and ADAM-SINDy methods is provided in Table 1, detailing the parametric values chosen for the comparative analysis.

3. Numerical Experiments

This section details the benchmark problems used in this study, encompassing five systems of nonlinear ordinary differential equations (ODEs) and a sixth case involving a nonlinear partial differential equation (PDE). The final test case highlights the advantages of integrating trainable sparsifying hyperparameters (λ) within the ADAM-SINDy framework. Each benchmark problem features a nonlinear parameter that poses challenges for the classical SINDy approach, and the SINDy-W method successfully identifies the governing dynamics for all cases as expected. These results underscore the challenges often encountered in practical SINDy applications (SINDy-W/o) when the correct nonlinear parameter is absent from the candidate library.

The results from ADAM-SINDy using batch-wise optimization are excluded, as this method failed to produce accurate outcomes for complex dynamical systems such as the pharmacokinetic model and wildfire PDE identification, where a batch size of approximately 70-80% of the entire dataset was required, making it nearly equivalent to full-batch optimization. Consequently, only the full-batch ADAM-SINDy results are presented here, as this approach yielded reliable and accurate solutions for all test cases.

3.1. Harmonic Oscillator — Fourier Frequency

First, we investigate Fourier frequencies within the candidate matrix by considering the harmonic oscillator as a benchmark problem. This system models a particle experiencing a restoring force proportional to its displacement from equilibrium. The dynamics of the system are governed by the following set of ODEs:

$$\begin{aligned} \dot{x} &= ay \, , \\ \dot{y} &= -bx + cy\cos(dx) \, , \end{aligned} \tag{9}$$

where $x(t)$ represents the displacement and $y(t)$ represents the velocity. The term bx corresponds to the linear restoring force as described by Hooke's law, while the cosine term introduces nonlinear effects through the frequency parameter d, which captures external factors such as damping or external driving forces. This example illustrates the effectiveness of the ADAM-SINDy framework in accurately computing the Fourier frequency d, as well as identifying other system coefficients, without the need for correct predefined parameter distributions, a limitation inherent to the classical SINDy approach. In this case, the cosine frequency d is set to 0.75, a non-integer value, while the other parameters are chosen as $a = 1$, $b = 1$, and $c = 0.1$, to represent the ground truth dynamics of the system, which is generated up to $t = 50$ with the initial condition of $x_0 = -2$ and $y_0 = 0$, for a time step of 0.01.

The results, depicted in Fig. 1, provide a comparative analysis of the governing equations corresponding to the ground truth system and those identified by the SINDy-W, SINDy-W/o, and ADAM-SINDy methodologies. While the classical SINDy-W/o method yielded a trajectory that closely matches the ground truth data, the identified system dynamics were unnecessarily complex and deviated from the true governing equations. In contrast, the ADAM-SINDy framework

Experiment			Harmonic Oscillator	Van der pol Oscillator	ABC Flow	Chemical Reaction	Pharmacokinetics Model
SINDy	SINDy - W	λ	0.01	0.0075	0.1	0.025	0.01
		$\mathcal{A}$	**1.0**	**1.0**, **2.15**	1.0	**1.0**	$\mathbf{X^{1.0}}$ $t^{(-0.4,\mathbf{-0.5},-0.55)}$
		$\mathcal{B},\mathcal{C},\mathcal{E},\mathcal{F}$	0.25, 0.5, **0.75**, 1.0	π	$\frac{\pi}{2},\frac{\pi}{\mathbf{2.8}},\frac{\pi}{3},\frac{\pi}{4},\frac{\pi}{\mathbf{4.5}},\frac{\pi}{5}$	π	π
		$\mathcal{D},\mathcal{G}$	1.0	1.0	1.0	1.0, **1.015** **1.025**, 2	1.0, 2.0
	SINDy - W/o	$\mathcal{A}$	1.0	1.0, 2.5	1.0	1.0	$\mathbf{X}^{1.0}$ $t^{(-0.4,-0.55)}$
		$\mathcal{B},\mathcal{C},\mathcal{E},\mathcal{F}$	0.2, 0.5, 0.7, 1.0	π	$\frac{\pi}{2},\frac{\pi}{2.5},\frac{\pi}{3.5},\frac{\pi}{4},\frac{\pi}{4.2},\frac{\pi}{5}$	π	π
		$\mathcal{D},\mathcal{G}$	1.0	1.0	1.0	1.0, 2.0	1.0, 2.0
ADAM-SINDy		Epochs	50000	32000	60000	40000	40000
		Initial learning rate	0.1	0.01	0.1	0.01	0.01
		Step decay epochs	4000	2500	4000	3000	4500

Table 1: Hyperparameters utilized in the classical SINDy methods (SINDy-W and SINDy-W/o) and the ADAM-SINDy method across the benchmark problems considered in this study. The nonlinear parameters $\mathcal{A},\mathcal{B},\mathcal{C},\mathcal{D},\mathcal{E},\mathcal{F},\mathcal{G}$ represent values employed in the library for the SINDy-W and SINDy-W/o approaches, demonstrating performance when the distributed range covers exact (SINDy-W) and approximate (SINDy-W/o) parameters of the system dynamics. Parameters in **bold** indicate exact values derived from the ground truth data in the SINDy-W method. For the pharmacokinetics model, $\mathcal{A}$ refers to the exponents used for the state variable and the time-dependent function, enumerated accordingly. Hyperparameters specific to the wildfire PDE example are discussed in the relevant section.
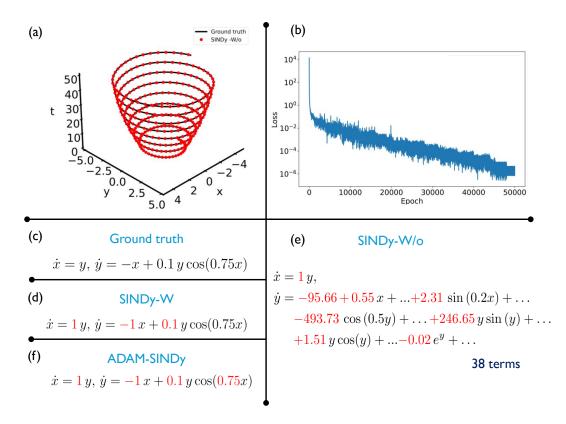
Figure 1: Harmonic oscillator example. (a) Temporal trajectory comparison showing both the ground truth and the SINDy-W/o method. (b) Loss plot illustrating the convergence behavior of the ADAM-SINDy method. A comparison of the governing equations is provided between the (c) ground truth and those identified by the (d) SINDy-W, (e) SINDy-W/o, and (f) ADAM-SINDy approaches. The red-highlighted numerical values indicate the optimized parameters obtained through these methodologies. For the SINDy-W/o method, a total of 38 terms were identified for $\dot{y}$, reflecting the complexity of the resulting dynamical system. Ground truth data is generated up to $t = 50$ with the initial conditions $x_0 = -2$ and $y_0 = 0$, using a time step of 0.01.

accurately computed the Fourier frequency and demonstrated a clear advantage by recovering the system's dynamics with greater accuracy, even in the presence of nonlinearity, as evidenced by quantitative analysis. SINDy-W also captures the true dynamical system, albeit by assuming precise knowledge of the frequency d in its library. It should be noted that in all figures the trajectory for SINDy-W and ADAM-SINDy methods are not shown as these methods identify the exact governing equations, therefore the trajectories are identical to the ground-truth.

3.2. Van der Pol Oscillator — Rational Exponent

This example focuses on the computation of rational exponents within the candidate matrix by employing the Van der Pol oscillator, a standard example of a nonlinear dynamical system characterized by self-sustained oscillations. The system is governed by the following set of first-order differential equations

$$\dot{x} = y \,,$$
$$\dot{y} = \mu(1 - x^b)y - x \,,$$
(10)

where the parameter μ introduces nonlinear damping, thereby influencing both the amplitude and frequency of the oscillations. For small values of μ, the system behaves similarly to a simple harmonic oscillator. However, as μ increases, the system's nonlinearity becomes more pronounced, leading to complex dynamics, including limit cycles with variable amplitude and frequency. The

primary objective in this example is for the ADAM-SINDy framework to accurately identify the exponent b in the nonlinear term, particularly when b takes on rational values, as opposed to the conventional integer value of 2. Accurately identifying such rational exponents poses significant challenges for classical SINDy methods, which often struggle with precise computation in these cases (unless the precise exponent is known in SINDy-W). The ground truth for this system is defined by choosing $\mu = 0.01$ and $b = 2.15$, with the non-integer exponent contributing to the system's complex nonlinear behavior, which is generated up to $t = 200$ with the initial condition of $x_0 = 0$ and $y_0 = -1$, for a time step of 0.01. In addition to the first-order polynomials in the candidate master library, the $\mathcal{A}$ parameter in Eq. 8 is made trainable in the ADAM-SINDy method to accommodate the chosen non-integer value, while a range of parameters $(1, 2.15)$ and $(1, 2.5)$ are selected for the classical SINDy-W and SINDy-W/o methodologies, respectively.

Fig. 2 presents a detailed comparison of the governing equations for the ground truth system and those identified by the SINDy-W, SINDy-W/o, and ADAM-SINDy methods. Although the SINDy-W/o method is able to align the trajectory with the ground truth data, it identifies a significantly more complex and dense equation compared to the original system. In contrast, the ADAM-SINDy framework demonstrates its ability to accurately compute the non-integer exponent b and other coefficients of the governing equations by self-adapting the exponent. This capability is particularly noteworthy, as it enables the ADAM-SINDy approach to correctly identify relevant terms within the system's governing equations, even when the exponent is a rational number. Consequently, the ADAM-SINDy framework provides a more parsimonious representation of the system dynamics, highlighting its efficacy in dealing with non-integer exponent values that are difficult to guess a priori in the library of candidate terms.

3.3. ABC Flow — Multiple Fourier Frequencies

In this section, we investigate the computation of multiple Fourier frequencies and amplitudes, focusing on the complex dynamics of an analytically defined chaotic fluid flow system. To facilitate this analysis, we examine the well-established benchmark problem known as the ABC (Arnold-Beltrami-Childress) flow, which is frequently employed to study intricate fluid dynamics and chaotic behavior in three-dimensional systems [54]. The velocity components of the ABC flow, which adhere to incompressibility, are formulated as follows:

$$
\begin{aligned}
\dot{x} &= A \sin\left(w_1 z\right) + C \cos\left(w_2 y\right) \ , \\
\dot{y} &= B \sin\left(w_3 x\right) + A \cos\left(w_4 z\right) \ , \\
\dot{z} &= C \sin\left(w_5 y\right) + B \cos\left(w_6 x\right) \ ,
\end{aligned}
\tag{11}
$$

where x, y, and z represent the spatial coordinates, A, B, and C denote the amplitudes, and w_i correspond to the frequencies.

The ABC flow gives rise to dynamic behaviors that range from simple periodic motions to complex, chaotic patterns, contingent on the specific parameters selected. A key characteristic of the ABC flow is its ability to produce intricate three-dimensional trajectories, making it a suitable model for examining chaotic dynamics in an autonomous dynamical system. Traditionally, the ABC flow has been modeled using a single Fourier frequency for simplicity. However, this work extends the analysis to encompass six distinct frequencies $w \in (\frac{\pi}{2}, \frac{\pi}{2.8}, \frac{\pi}{3}, \frac{\pi}{4}, \frac{\pi}{4.5}, \frac{\pi}{5})$, with Fourier amplitudes of $A = 2$, $B = 3$, and $C = 1$, for which the ground truth generated up to $t = 20$ with the initial conditions $x_0 = 0.5$, $y_0 = 0.2$, and $z_0 = 1.0$, using a time step of 0.01. In this multi-frequency context, both the SINDy-W and SINDy-W/o methods require an expanded candidate library, rendering the identification process more computationally intensive. By contrast, the ADAM-SINDy framework efficiently identifies all the Fourier frequencies and their corresponding

(a)

Ground truth
SINDy -W/o

t

(b)

Loss

Epoch

(c) Ground truth

$$\dot{x} = y, \; \dot{y} = 0.01 \left(1 - x^{2.15}\right) y - x$$

(d) SINDy-W

$$\dot{x} = 1.0\,y, \; \dot{y} = 0.01 \left(1 - x^{2.15}\right) y - 1\,x$$

(f) ADAM-SINDy

$$\dot{x} = 0.4417\,y + 0.5583\,y e^{0.00\,y} = 1.0\,y,$$
$$\dot{y} = 0.01\,y - 0.01\,x^{2.15}\,y - 1.0\,x$$

(e) SINDy-W/o

$$\dot{x} = 1.0\,y,$$
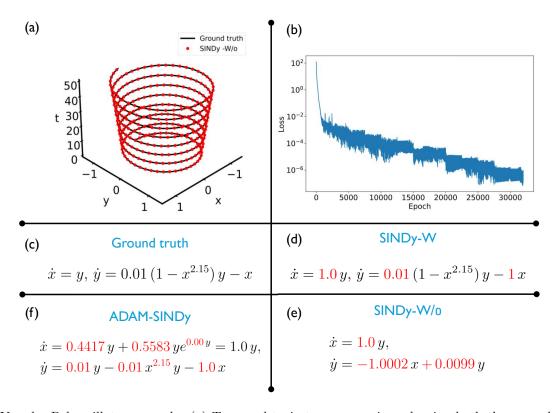$$\dot{y} = -1.0002\,x + 0.0099\,y$$

Figure 2: Van der Pol oscillator example. (a) Temporal trajectory comparison showing both the ground truth and the SINDy-W/o method. (b) Loss plot illustrating the convergence behavior of the ADAM-SINDy method. A comparison of the governing equations is provided between the (c) ground truth and those identified by the (d) SINDy-W, (e) SINDy-W/o, and (f) ADAM-SINDy approaches. The red-highlighted numerical values indicate the optimized parameters obtained through these methodologies. Ground truth data is generated up to $t = 200$ with the initial conditions $x_0 = 0$ and $y_0 = -1$, using a time step of 0.01.

amplitudes as illustrated in Fig. 3. As anticipated, the SINDy-W method successfully identifies all six Fourier frequencies and amplitudes. However, the SINDy-W/o method generates a complex and dense dynamical system equation that diverges significantly from the ground truth data, failing to produce accurate results despite including three correct frequencies among the six if the remaining three frequencies are incorrect. This underscores the importance of optimizing nonlinear parameters, positioning ADAM-SINDy as a robust and effective tool for identifying intricate dynamical systems such as the multi-frequency ABC flow.

Additionally, a supplementary experiment was conducted to explore the potential of utilizing the computational graph inherent to stochastic gradient descent (PyTorch environment) by employing $\boldsymbol{\Gamma}$ as a differential divergence operator, rather than as a scaling matrix for individual candidates. In fluid dynamics, ensuring a divergence-free velocity field, which aligns with the conservation of mass, is a critical constraint. By embedding this physical principle into the optimization process, ADAM-SINDy applies $\boldsymbol{\Gamma}$ as a divergence operator, thereby enforcing adherence to the continuity equation. This novel approach enables the identification of all six Fourier frequencies and their corresponding amplitudes within just 20 epochs, a substantial reduction in computational effort compared to the standard ADAM-SINDy method, which typically requires around 60,000 epochs when $\boldsymbol{\Gamma}$ is treated as a scaling matrix. This preliminary investigation suggests the potential for a physics-informed SINDy approach, which diverges from the primary focus of the current study and will be pursued in future work.

3.4. Chemical Reaction Kinetics — Exponential Exponent

Next, the computation of an exponential exponent within a dynamical system is examined through a chemical reaction kinetics problem that employs an exponential approximation of the Arrhenius rate law, which characterizes the nonlinear relationship between reaction rates and temperature, particularly in the context of coupled first-order reactions [55]. When the temperature increase due to an exothermic reaction is negligible compared to the ambient temperature, the reaction rate can be approximated as exponentially dependent on this incremental temperature change. By appropriately scaling the governing equations for mass and energy, the system is expressed as follows [55]

$$
\begin{aligned}
\dot{\alpha} &= -k\alpha e^{g\theta} + \mu \ , \\
\dot{\theta} &= \alpha e^{h\theta} - \theta \ ,
\end{aligned}
\tag{12}
$$

where $\alpha(t)$ represents the concentration of an intermediate reactant, $\theta(t)$ denotes the temperature rise, k is the reaction rate constant, and μ corresponds to the reactant concentration. The model assumes that the states θ and α evolve on a faster time scale compared to the slowly changing reactant consumption μ, invoking the pseudo-stationary-state hypothesis [56], thus μ interacting as a constant source term. This formulation offers insights into the temporal evolution of reactant concentrations and temperature, enabling the analysis of reaction kinetics and the impact of external perturbations on the reaction system.

Conventionally, the growth/decay rates g and h are assumed to be unity for the system under consideration [55, 56]. However, this experiment adopts non-integer values for the parameters, specifically $g = 1.015$ and $h = 1.025$, while setting $k = 0.07$ and $\mu = 0.1$ to generate the ground truth data up to $t = 200$ with initial conditions $\alpha_0 = 0$ and $\theta_0 = 5$ using a time step of 0.02. Fig. 4 provides a comprehensive comparison of the classical SINDy-W, SINDy-W/o, and ADAM-SINDy methods in identifying the chemical reaction system. In this context, the SINDy-W/o method exhibits deviation from the ground truth trajectory at α close to zero, failing to accurately replicate the dynamics. In contrast, the ADAM-SINDy method successfully identifies the non-integer exponent values and
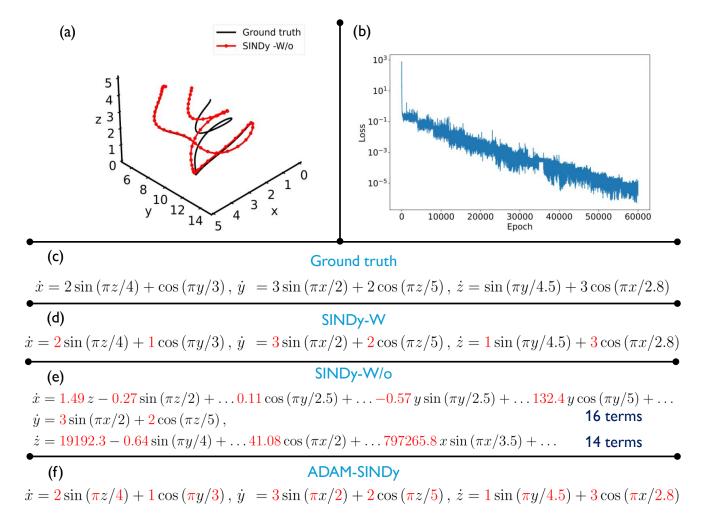
(a)

(b)

(c) Ground truth

$$\dot{x} = 2\sin\left(\pi z/4\right) + \cos\left(\pi y/3\right), \; \dot{y} = 3\sin\left(\pi x/2\right) + 2\cos\left(\pi z/5\right), \; \dot{z} = \sin\left(\pi y/4.5\right) + 3\cos\left(\pi x/2.8\right)$$

(d) SINDy-W

$$\dot{x} = 2\sin\left(\pi z/4\right) + 1\cos\left(\pi y/3\right), \; \dot{y} = 3\sin\left(\pi x/2\right) + 2\cos\left(\pi z/5\right), \; \dot{z} = 1\sin\left(\pi y/4.5\right) + 3\cos\left(\pi x/2.8\right)$$

(e) SINDy-W/o

$$\dot{x} = 1.49\,z - 0.27\sin\left(\pi z/2\right) + \ldots 0.11\cos\left(\pi y/2.5\right) + \ldots -0.57\,y\sin\left(\pi y/2.5\right) + \ldots 132.4\,y\cos\left(\pi y/5\right) + \ldots$$

$$\dot{y} = 3\sin\left(\pi x/2\right) + 2\cos\left(\pi z/5\right),$$ **16 terms**

$$\dot{z} = 19192.3 - 0.64\sin\left(\pi y/4\right) + \ldots 41.08\cos\left(\pi x/2\right) + \ldots 797265.8\,x\sin\left(\pi x/3.5\right) + \ldots$$ **14 terms**

(f) ADAM-SINDy

$$\dot{x} = 2\sin\left(\pi z/4\right) + 1\cos\left(\pi y/3\right), \; \dot{y} = 3\sin\left(\pi x/2\right) + 2\cos\left(\pi z/5\right), \; \dot{z} = 1\sin\left(\pi y/4.5\right) + 3\cos\left(\pi x/2.8\right)$$

Figure 3: ABC flow example. (a) Pathline trajectory comparison showing both the ground truth and the SINDy-W/o method. (b) Loss plot illustrating the convergence behavior of the ADAM-SINDy method. A comparison of the governing equations is provided between the (c) ground truth and those identified by the (d) SINDy-W, (e) SINDy-W/o, and (f) ADAM-SINDy approaches. Optimized parameter values, highlighted in red, indicate results obtained through these methodologies. For the SINDy-W/o method, a total of 16 and 14 terms were identified for $\dot{x}$ and $\dot{z}$, reflecting the complexity of the derived dynamical system. In the ADAM-SINDy method, all optimized Fourier frequency values are approximated to 16 decimal places, consistently aligning with the value of π. Ground truth data is generated up to $t = 20$ with the initial conditions $x_0 = 0.5$, $y_0 = 0.2$, and $z_0 = 1.0$, using a time step of 0.01.
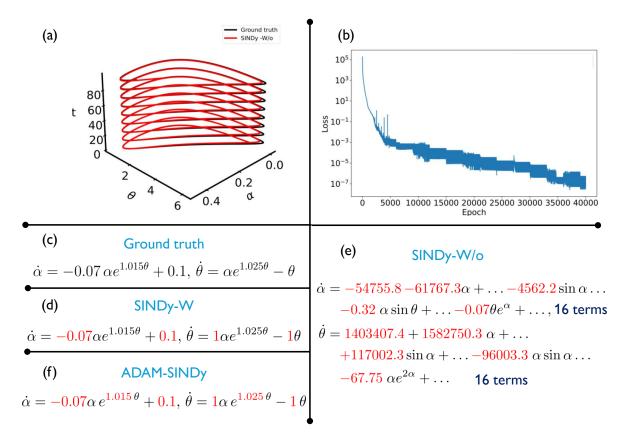
Figure 4: Chemical reaction kinetics example. (a) Temporal trajectory comparison showing both the ground truth and the SINDy-W/o method. (b) Loss plot demonstrating the convergence behavior of the ADAM-SINDy method. A comparison of the governing equations is provided between the (c) ground truth and those identified by the (d) SINDy-W, (e) SINDy-W/o, and (f) ADAM-SINDy approaches. The optimized parameters, highlighted in red, represent the results obtained from these methodologies. For the SINDy-W/o method, a total of 16 terms were identified for both $\dot{\alpha}$ and $\dot{\theta}$, indicating the complexity of the resulting dynamical system. Ground truth data is generated up to $t = 200$ with the initial conditions $\alpha_0 = 0$ and $\theta_0 = 5$, using a time step of 0.02.

other relevant coefficients perfectly aligning with the ground truth data, thereby demonstrating its efficacy in addressing systems characterized by exponential functions.

3.5. Pharmacokinetics Model — Time-dependent Reaction

This example investigates a dynamical system that incorporates a time-dependent function with a non-integer exponent in its governing equations, focusing on a pharmacokinetics model. Such models are commonly utilized to assess the rate of drug concentration across various compartments in the human body. Specifically, we consider a single-dose compartmental model [57] governed by the following system of equations:

$$
\begin{aligned}
k_g &= k_0 t^{-\eta} \ , \\
\dot{B} &= k_g G - k_b B \ , \\
\dot{G} &= -k_g G \ , \\
\dot{U} &= k_b B \ ,
\end{aligned}
\tag{13}
$$

where k_g denotes the time-dependent reaction rate [58], k_0 is the initial rate coefficient, and η represents the fractal kinetics exponent, constrained within the range $0 < \eta < 1$. The ground truth

data are generated using a drug absorption rate of $k_b = 0.15$, $k_0 = 0.72$, and a fractal kinetics exponent of $\eta = -0.5$, evolved up to $t = 10$ with the initial conditions $B_0 = 0$, $G_0 = 1$, and $U_0 = 0$ for a time step of 0.001.

In this example, the master library is expanded to include $\mathbf{X} \otimes t^\eta$, thereby accommodating the time-dependent function, with η treated as a trainable parameter within the ADAM-SINDy framework, while a range of parameters $(-0.4, -0.5, -0.55)$ and $(-0.4, -0.55)$ are defined for the SINDy-W and SINDy-W/o methodologies, respectively. Fig. 5 presents a detailed comparison of the governing equations for the ground truth system with those identified by the SINDy-W, SINDy-W/o, and ADAM-SINDy methodologies. Notably, the SINDy-W/o method closely aligns with the ground truth trajectory, exhibiting no deviations. However, the resulting equation from this method is significantly more complex and dense compared to the original system. In contrast, the ADAM-SINDy framework accurately computes the exponent η associated with the temporal function, along with other coefficients, mirroring the governing system precisely and thereby demonstrating superior performance compared to the classical SINDy methods.

3.6. Wildfire Transport - Partial Differential Equation

The classical SINDy method was initially developed to discover systems of ODEs but has been extended to encompass PDEs through a process known as PDE-FIND [59]. This extension is particularly pertinent for systems exhibiting dependencies in both spatial and temporal domains. In this section, we investigate wildfire dynamics modeled by PDEs, focusing on the identification of governing nonlinear parameters that elucidate the spatiotemporal evolution of temperature within the fire. These governing equations encapsulate critical processes, including heat transfer, combustion, and the influence of wind, thereby providing a comprehensive framework for understanding wildfire propagation across various fuel beds. The following wildfire combustion model [60] delineates this behavior, incorporating terms for advection, linear diffusion, reaction, and natural cooling:

$$\frac{\partial T}{\partial t} + \overrightarrow{\mathbf{V}} \cdot \nabla T = \kappa \nabla^2 T + \beta \mathrm{e}^{T/(1+\epsilon T)} - \alpha T , \tag{14}$$

where $T(\mathbf{x}, t)$ denotes the non-dimensionalized absolute temperature, $\overrightarrow{\mathbf{V}}$ represents the normalized velocity vector of the fire front, κ is the normalized thermal diffusivity, β denotes the fuel mass fraction, ϵ is the inverse activation energy, and α represents the natural heat transfer coefficient. For this experiment, we consider the candidate matrix

$$\boldsymbol{\Theta} = \begin{bmatrix} 1 & \mathbf{X} & \nabla \mathbf{X} & \nabla^2 \mathbf{X} & \nabla^3 \mathbf{X} & \nabla^4 \mathbf{X} & \exp\left(\frac{\mathbf{X}}{1 + \mathcal{H}\mathbf{X}}\right) \end{bmatrix} , \tag{15}$$

which incorporates a diverse range of candidate functions. This matrix includes polynomials up to the first order, as well as an exponential term with $\mathcal{H}$ serving as an unknown optimizable parameter, consistent with Arrhenius' law—typically employed in modeling fuel combustion processes. Additionally, it encompasses higher-order partial spatial derivatives, extending to the fourth derivative.

The ground truth data is generated by employing an upwind compact scheme for spatial derivatives and implicit-explicit Runge-Kutta time integration within the finite difference method, where the initial Heaviside firefront is situated at coordinates $(8.0, 8.0)$ with a square side length of 4, computed up to $t = 0.08$ with a time step of 10^{-7}. The dimensionless parameters include a north-east facing freestream velocity magnitude of 10, a linear diffusion coefficient $k = 1.1$, an inverse activation energy $\epsilon = 0.3$, a fuel $\beta = 1$ and a natural heat transfer coefficient $\alpha = 0.20$. In the context of the SINDy-W and SINDy-W/o methods, we consider the sets $\mathcal{H} \in \{0.2, 0.3, 0.4\}$ and $\{0.2, 0.4\}$
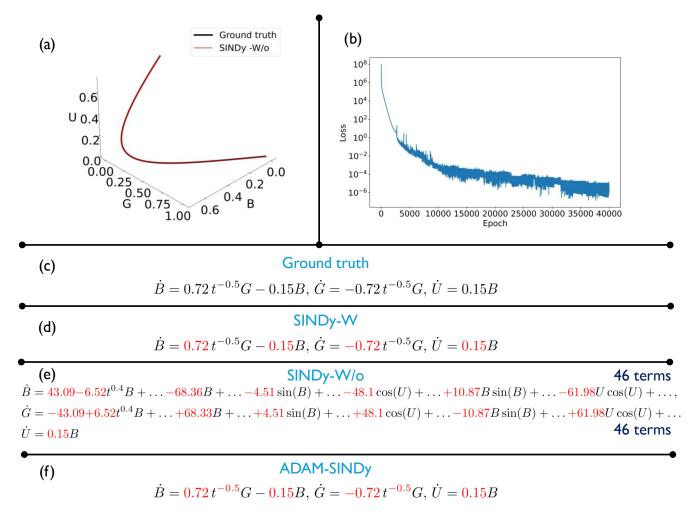
Figure 5: Pharmacokinetics example. (a) Temporal trajectory comparison highlighting both the ground truth and the SINDy-W/o method. (b) Loss plot illustrating the convergence behavior of the ADAM-SINDy method. A comparison of the governing equations is provided between the (c) ground truth and those identified by the (d) SINDy-W, (e) SINDy-W/o, and (f) ADAM-SINDy approaches. The optimized parameters, highlighted in red, reflect the outcomes of these methodologies. For the SINDy-W/o method, a total of 46 terms were identified for both $\dot{B}$ and $\dot{G}$, indicating the complexity of the resulting dynamical system. Ground truth data is generated up to $t = 10$ with the initial conditions $B_0 = 0$, $G_0 = 1$, and $U_0 = 0$, using a time step of 0.001.
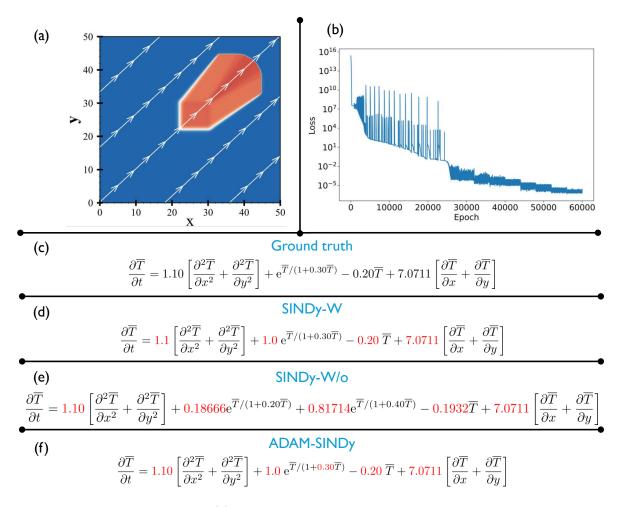
Figure 6: Wildfire dynamics example. (a) Ground truth temperature data superimposed with north-east facing wind streamlines at $t = 0.05$. (b) Loss plot illustrating the convergence behavior of the ADAM-SINDy method. A comparison of the governing equations is provided between the (c) ground truth and those identified by the (d) SINDy-W, (e) SINDy-W/o, and (f) ADAM-SINDy approaches. Optimized parameters, highlighted in red, indicate the results obtained through these methodologies. The initial Heaviside firefront is situated at coordinates $(8.0, 8.0)$ with a square side length of 4, computed up to $t = 0.08$ with a time step of 10^{-7}.

for the identification of the wildfire equation, with the sparsity parameter set to $\lambda = 0.01$. Figure 6 illustrates a detailed comparison of the governing equations for the ground truth system with those identified by the SINDy-W, SINDy-W/o, and ADAM-SINDy methodologies. As anticipated, the SINDy-W/o method identifies an overly complex and dense wildfire model in comparison to the ground truth system. Interestingly, the ADAM-SINDy framework accurately identifies the exact wildfire combustion model, perfectly predicting the inverse activation energy associated with the reaction term.

3.7. Hyperparameter Robustness — Sparsity Knob λ

In this section, we investigate the optimization efficacy of the ADAM-SINDy framework in system identification by studying the effect of the sparsity-promoting parameters. To simplify the comparison with classical SINDy, $\mathbf{\Gamma}$ was fixed as the identity matrix, and the scalar λ was made trainable. To study the sensitivity to this hyperparameter, an experiment using the SINDy-W method was conducted. By systematically adjusting the λ parameter from smaller to larger values, the goal was to identify the threshold at which the model begins to diverge significantly from the
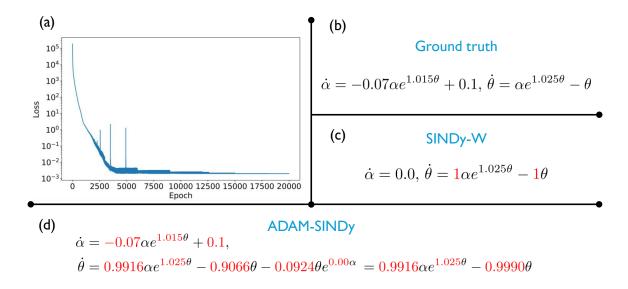
(a)

(b) Ground truth

$$\dot{\alpha} = -0.07\alpha e^{1.015\theta} + 0.1, \; \dot{\theta} = \alpha e^{1.025\theta} - \theta$$

(c) SINDy-W

$$\dot{\alpha} = 0.0, \; \dot{\theta} = 1\alpha e^{1.025\theta} - 1\theta$$

(d) ADAM-SINDy

$$\dot{\alpha} = -0.07\alpha e^{1.015\theta} + 0.1,$$
$$\dot{\theta} = 0.9916\alpha e^{1.025\theta} - 0.9066\theta - 0.0924\theta e^{0.00\alpha} = 0.9916\alpha e^{1.025\theta} - 0.9990\theta$$

Figure 7: The influence of the sparsity knob (λ) on chemical reaction kinetics results. (a) Loss plot showing the convergence of the ADAM-SINDy method for λ_{max}. A comparison of the governing equations is provided between the (b) ground truth and those identified by the (c) SINDy-W and (d) ADAM-SINDy approaches, for $\lambda_{\mathrm{max}} = 0.1$. The red-highlighted numerical values indicate the optimized parameters obtained.

ground truth. The objective was to estimate the minimum λ (λ_{min}), below which the SINDy-W method generates an overly dense system of equations and the maximum λ (λ_{max}), beyond which the model fails to capture meaningful dynamics. In ADAM-SINDy, λ was initialized with these minimum and maximum threshold values and made trainable. All numerical experiments consistently demonstrated robust performance at the λ_{max} initialized value, highlighting the ADAM-SINDy framework's robustness. A notable example is the chemical kinetics problem, illustrated in Fig. 7 that demonstrates the robustness of ADAM-SINDy compared to SINDy-W, where the estimated values for λ_{max} and λ_{min} are 0.1 and 0.001, respectively. It could be seen that SIND-W can no longer produce the ground-truth equation when λ_{max} was used, whereas ADAM-SINDy is more robust when initialized with λ_{max}. Furthermore, when λ_{min} was used, both the SINDy-W and ADAM-SINDy methods failed (results not shown). This observation suggests that ADAM-SINDy demonstrates enhanced robustness in the selection of the sparsifying hyperparameter, particularly when initialized with larger values.

4. Discussion

Identification of nonlinear dynamical systems is a prominent research domain that plays a pivotal role in elucidating the underlying physics of various problems. The literature highlights extensive investigations that employ the SINDy and symbolic regression frameworks, both of which can identify governing equations from observational data. However, it is essential to recognize that these well-established methods possess distinct advantages and disadvantages, particularly concerning computational optimization. In this context, the newly developed ADAM-SINDy framework emerges at the intersection of these established approaches, leveraging their computational optimization benefits. By employing the ADAM optimization algorithm, ADAM-SINDy facilitates the simultaneous optimization of parameters and coefficients associated with candidate nonlinear functions. This innovative approach enables more efficient and accurate parameter estimation without the necessity for prior knowledge of nonlinear characteristics, such as frequencies in trigonometric

functions or bandwidths in exponential functions. A key factor in ADAM-SINDy's success lies in its ability to exploit the computational graph inherent in the gradient descent algorithm implementation in the PyTorch environment. This structure facilitates efficient backpropagation of gradients, enabling dynamic interaction between candidate terms and nonlinear parameters during the optimization process. By allowing the model to adaptively refine both the nonlinear parameters and coefficients, ADAM-SINDy enhances the robustness and precision of system identification, particularly in complex dynamical systems where the classical SINDy method struggles with sparse, non-convex landscapes. Notably, the strategy behind the simultaneous optimization of all unknown parameters and coefficients closely parallels the use of adaptive activation functions [61] in neural network research, where the parameters of nonlinear adaptive activation functions, along with the weights and biases of linear layers, are optimized concurrently.

Interestingly, the ADAM-SINDy framework also facilitates interaction among the functions within the candidate library through the self-adaptation of nonlinear functions. This self-adaptive mechanism significantly enhances the model's capacity to capture complex dynamical behaviors, thereby allowing it to adjust to the varying degrees of nonlinearity inherent in real-world systems. Such adaptability is particularly crucial when predefined candidates are lacking, as it optimizes parameters to compensate for absent functions. In contrast, the classical SINDy approach is constrained by static nonlinear parameters and a lack of interaction, increasing the risk of inaccurate system models when essential candidate functions are omitted. This adaptability parallels the advantages observed in symbolic regression techniques, further enriching the model's applicability. Concurrently, ADAM-SINDy aims to identify a parsimonious and elegant mathematical model by incorporating essential computational methodologies, such as L1-norm loss functions and sequential thresholding, which are crucial for the success of the classical SINDy method. Furthermore, a distinct advantage of ADAM-SINDy lies in the optimization of sparsity-promoting hyperparameters such as Γ. This optimization strategy reduces the need for extensive manual tuning, thereby enhancing the model's robustness. This trainable Γ further advances the Adaptive LASSO method, by enabling the dynamic imposition of candidate-specific penalties during the optimization process, leading to a "fully" adaptive LASSO approach. Such adaptive weighting/scaling flexibility is particularly advantageous in applications involving high-dimensional datasets, as it reduces the risk of overfitting while simultaneously enhancing the interpretability of the model. While ADAM-SINDy offers both batch-wise and full-batch optimization, it has been observed that for simpler dynamical systems, a small randomly sampled batch of data is often sufficient to capture the necessary temporal information for accurately estimating governing parameters. However, for more complex systems, a small batch may not encompass all required information, necessitating a larger batch size that ideally approaches full-batch size. Consequently, full-batch optimization is preferred and utilized in the present work, leading to reduced uncertainty in the converged optimized parameters within the ADAM-SINDy methodology.

Ultimately, the integrated simultaneous adaptive optimization of the parameters of nonlinear candidate functions, coefficients of the candidate matrix, and hyperparameters based on training data positions ADAM-SINDy as a powerful and effective tool for modeling a diverse range of dynamical behaviors across various applications. The proposed ADAM-SINDy methodology is thoroughly investigated across a wide spectrum of dynamical systems, including benchmark coupled ODEs such as oscillators, fluid flows, reaction kinetics, and wildfire dynamics PDE. These comprehensive investigations demonstrated its efficacy in accurately computing nonlinear features such as multiple Fourier frequencies, non-integer exponents in polynomials, and exponential exponents. Furthermore, the investigation also explored the inherent limitations of the classical SINDy method, illustrating its consistent failure to identify the exact model when the precise parameters are absent

from the candidate matrix. This comprehensive investigation highlights the considerable potential of the ADAM-SINDy optimization framework, thereby extending its applicability to the modeling of intricate and diverse dynamical systems across various contexts with limited prior knowledge.

It is worth noting that recent advancements in symbolic regression via neural networks have focused on identifying dynamical systems [55]. Boddupalli et al. [55] applied this approach to chemical reaction kinetics, the same system considered in our work (Sec. 3.4), and their results produced overly complex, "bloated" equations characterized by cubic polynomials nonlinearly combined with exponential functions [55]. While the inclusion of stacked exponential terms alongside polynomials was necessary for convergence, it significantly increased model complexity, leading to inaccuracies in predicting the true trajectory and governing dynamics [55]. In contrast to the considered growth rates of unity for reactant concentration and temperature [55, 56], we applied ADAM-SINDy to the same chemical reaction system (see Fig. 4), tackling a more computationally challenging scenario involving nonlinear parameter estimation with non-integer rational exponents of 1.015 and 1.025 for reactant concentration and temperature, respectively. Remarkably, ADAM-SINDy accurately identified the true dynamical system, capturing both slow and fast transients without requiring additional treatments to ensure regression convergence.

In real-world problems, the presence of noise in the observational data from various sources is inevitable, prompting an investigation into the efficacy of the ADAM-SINDy method. To assess its robustness against noisy data, we compared the ADAM-SINDy methodology to the classical SINDy-W method by applying Gaussian white noise of up to 50% of the standard deviation to all the numerical example datasets. However, the results from these noise level experiments were not presented in this paper, as both methods demonstrated similar performance and failed to exhibit advantages at high noise levels. Both methods performed effectively at lower noise levels, reinforcing the notion that neither method outperforms the other in the presence of significant noise. Future work will focus on further improving the ADAM-SINDy method to achieve superior performance under noisy conditions.

Furthermore, it is essential to acknowledge a notable limitation of the full batch-ADAM-SINDy methodology: its inherent computational expense due to the utilization of the ADAM optimization algorithm for the coefficient matrix. Although this approach offers significant advantages over the classical SINDy method, it incurs a considerable computational cost. This cost arises despite the fact that the ADAM-SINDy method mirrors all computational strategies of its predecessor, differing primarily in the employed optimization algorithm. Efficiency can be achieved by integrating an iterative least squares method for optimizing the coefficient matrix while utilizing the ADAM optimizer for nonlinear parameters and sparsity knobs, leading to a combined least-squares-ADAM optimization framework for system identification. However, integrating these approaches presents challenges, particularly in ensuring compatibility between the iterative least squares method and the ADAM optimizer. Achieving seamless integration requires addressing potential conflicts between sparsity constraints and nonlinear optimization objectives. Consequently, further research is essential to develop robust methodologies that can effectively merge these distinct approaches while preserving the desirable properties of each. Additionally, one can explore the efficacy of different algorithms, including variations of ADAM, to assess their performance in this context.

In the context of the ABC flow example, efforts were made to leverage the computational graph of the gradient descent algorithm by incorporating a divergence-free constraint into the loss equation. This approach demonstrated a noteworthy reduction in the total number of epochs required for optimization—approximately 20 epochs—compared to the typical requirement of around 6×10^4 epochs. This observation highlights the potential for further enhancement of the method in future work. Thus, a promising direction for future research involves exploring differential operator-based

sparsity controllers ($\mathbf{\Gamma}$). Such advancements could facilitate the development of a more parsimonious and interpretable dynamical system model that aligns with underlying physical laws, thereby significantly improving the computational efficacy of the ADAM-SINDy framework.

5. Conclusion

In summary, the proposed ADAM-SINDy methodology successfully addresses the limitations of the classical SINDy framework by enabling simultaneous identification of both system nonlinear parameters and coefficients through ADAM optimization. By eliminating the need for predefined parameter distributions and extensive manual hyperparameter tuning, ADAM-SINDy enhances the efficiency, adaptability, and robustness of system identification, particularly in the presence of nonlinear parameters. The demonstrated improvements across diverse dynamical systems highlight the potential of this approach to significantly broaden the applicability of the SINDy framework in complex modeling challenges.

Conflict of Interest

The authors declare no conflict of interest.

Acknowledgments

Data Availability

The ADAM-SINDy framework, developed in a PyTorch environment, will be made available on GitHub following the peer review process.

References

[1] L. Ljung, Perspectives on system identification, Annual Reviews in Control 34 (2010) 1–12.

[2] P. O. Van, B. M. De, Subspace identification for linear systems: Theory—Implementation—Applications, Springer Science & Business Media, 2012.

[3] O. Nelles, Nonlinear dynamic system identification, Springer, 2020.

[4] F. Lauer, G. Bloch, Hybrid system identification: Theory and algorithms for learning switching models, volume 478, Springer, 2018.

[5] P. F. Pai, A. N. Palazotto, HHT-based nonlinear signal processing method for parametric and non-parametric identification of dynamical systems, International Journal of Mechanical Sciences 50 (2008) 1619–1635.

[6] S. N. Kumpati, P. Kannan, Identification and control of dynamical systems using neural networks, IEEE Transactions on neural networks 1 (1990) 4–27.

[7] J. A. K. Suykens, J. P. L. Vandewalle, B. L. M. De, Artificial neural networks for modeling and control of non-linear systems, Springer Science & Business Media, 2012.

[8] A. C. Gondhalekar, E. P. Petrov, M. Imregun, Parameters Identification for Nonlinear Dynamic Systems Via Genetic Algorithm Optimization, Journal of Computational and Nonlinear Dynamics 4 (2009) 041002.

[9] M. Quade, M. Abel, K. Shafi, R. K. Niven, B. R. Noack, Prediction of dynamical systems by symbolic regression, Physical Review E 94 (2016) 012214.

[10] G.-J. Both, S. Choudhury, P. Sens, R. Kusters, DeepMoD: Deep learning for model discovery in noisy data, Journal of Computational Physics 428 (2021) 109985.

[11] A. Okunev, E. Burnaev, J. Wang, Ordinary differential equation identification based on sparse bayesian learning and collaborative neurodynamic optimization, in: 2021 6th International Conference on Communication, Image and Signal Processing (CCISP), IEEE, 2021, pp. 75–79.

[12] A. Okunev, E. Burnaev, Nonlinear system identification via sparse bayesian regression based on collaborative neurodynamic optimization, Journal of Inverse and Ill-posed Problems (2024).

[13] R. Stephany, C. Earls, PDE-READ: Human-readable partial differential equation discovery using deep learning, Neural Networks 154 (2022) 360–382.

[14] P. Rajendra, V. Brahmajirao, Modeling of dynamical systems through deep learning, Biophysical Reviews 12 (2020) 1311–1320.

[15] W. Samek, G. Montavon, S. Lapuschkin, C. J. Anders, K. R. Müller, Explaining deep neural networks and beyond: A review of methods and applications, Proceedings of the IEEE 109 (2021) 247–278.

[16] A. Thampi, Interpretable AI: Building explainable machine learning systems, Simon and Schuster, 2022.

[17] X. Zhong, B. Gallagher, S. Liu, B. Kailkhura, A. Hiszpanski, T. Y. J. Han, Explainable machine learning in materials science, Npj Computational Materials 8 (2022) 204.

[18] J. R. Koza, Genetic programming as a means for programming computers by natural selection, Statistics and computing 4 (1994) 87–112.

[19] J. Bongard, H. Lipson, Automated reverse engineering of nonlinear dynamical systems, Proceedings of the National Academy of Sciences 104 (2007) 9943–9948.

[20] M. Schmidt, H. Lipson, Symbolic regression of implicit equations, in: Genetic programming theory and practice VII, Springer, 2009, pp. 73–85.

[21] G. Dick, Bloat and generalisation in symbolic regression, in: Asia-Pacific Conference on Simulated Evolution and Learning, Springer, 2014, pp. 491–502.

[22] T. Sauer, J. A. Yorke, M. Casdagli, Embedology, Journal of Statistical Physics 65 (1991) 579–616.

[23] F. Takens, Detecting strange attractors in turbulence, in: Dynamical Systems and Turbulence, Warwick 1980: Proceedings of a Symposium held at the University of Warwick 1979/80, Springer, 2006, pp. 366–381.

[24] J. B. Tenenbaum, V. D. Silva, J. C. Langford, A global geometric framework for nonlinear dimensionality reduction, Science 290 (2000) 2319–2323.

[25] A. Singer, R. Erban, I. G. Kevrekidis, R. R. Coifman, Detecting intrinsic slow variables in stochastic dynamical systems by anisotropic diffusion maps, Proceedings of the National Academy of Sciences 106 (2009) 16090–16095.

[26] S. T. Roweis, L. K. Saul, Nonlinear dimensionality reduction by locally linear embedding, Science 290 (2000) 2323–2326.

[27] T. McConaghy, FFX: Fast, scalable, deterministic symbolic regression technology, Genetic Programming Theory and Practice IX (2011) 235–260.

[28] B. Burlacu, G. Kronberger, M. Kommenda, Operon C++ an efficient genetic programming framework for symbolic regression, in: Proceedings of the 2020 Genetic and Evolutionary Computation Conference Companion, 2020, pp. 1562–1570.

[29] G. Kronberger, L. Kammerer, M. Kommenda, Identification of dynamical systems using symbolic regression, in: Computer Aided Systems Theory–EUROCAST 2019: 17th International Conference, Las Palmas de Gran Canaria, Spain, February 17–22, 2019, Revised Selected Papers, Part I 17, Springer, 2020, pp. 370–377.

[30] M. Schmidt, H. Lipson, Distilling free-form natural laws from experimental data, Science 324 (2009) 81–85.

[31] H. Oh, R. Amici, G. Bomarito, S. Zhe, R. M. Kirby, J. Hochhalter, Inherently interpretable machine learning solutions to differential equations, Engineering with Computers 40 (2024) 2349–2361.

[32] W. Wang, R. Yang, Y. Lai, V. Kovanis, C. Grebogi, Predicting catastrophes in nonlinear dynamical systems by compressive sensing, Physical review letters 106 (2011) 154101.

[33] H. Schaeffer, R. Caflisch, C. D. Hauck, S. Osher, Sparse dynamics for partial differential equations, Proceedings of the National Academy of Sciences 110 (2013) 6634–6639.

[34] S. L. Brunton, J. L. Proctor, J. N. Kutz, Discovering governing equations from data by sparse identification of nonlinear dynamical systems, Proceedings of the national academy of sciences 113 (2016) 3932–3937.

[35] J. Loiseau, S. L. Brunton, Constrained sparse galerkin regression, Journal of Fluid Mechanics 838 (2018) 42–67.

[36] M. Dam, M. Brøns, J. Juul Rasmussen, V. Naulin, J. S. Hesthaven, Sparse identification of a predator-prey system from simulation data of a convection model, Physics of Plasmas 24 (2017).

[37] S. Beetham, J. Capecelatro, Formulating turbulence closures using sparse regression with embedded form invariance, Physical Review Fluids 5 (2020) 084611.

[38] A. A. Kaptanoglu, L. Zhang, Z. G. Nicolaou, U. Fasel, S. L. Brunton, Benchmarking sparse system identification with low-dimensional chaos, Nonlinear Dynamics 111 (2023) 13143–13164.

[39] L. Boninsegna, F. Nüske, C. Clementi, Sparse learning of stochastic dynamical equations, The Journal of Chemical Physics 148 (2018).

[40] E. Kaiser, J. N. Kutz, S. L. Brunton, Sparse identification of nonlinear dynamics for model predictive control in the low-data limit, Proceedings of the Royal Society A 474 (2018) 20180335.

[41] K. Kaheman, J. N. Kutz, S. L. Brunton, Sindy-pi: a robust algorithm for parallel implicit sparse identification of nonlinear dynamics, Proceedings of the Royal Society A 476 (2020) 20200279.

[42] P. Goyal, P. Benner, Discovery of nonlinear dynamical systems using a runge–kutta inspired dictionary-based sparse regression approach, Proceedings of the Royal Society A 478 (2022) 20210883.

[43] A. Arzani, L. Yuan, P. Newell, B. Wang, Interpreting and generalizing deep learning in physics-based problems with functional linear models, Engineering with Computers (2024) 1–23.

[44] A. A. Kaptanoglu, J. L. Callaham, A. Aravkin, C. J. Hansen, S. L. Brunton, Promoting global stability in data-driven models of quadratic nonlinear dynamics, Physical Review Fluids 6 (2021) 094401.

[45] J. L. Callaham, J. C. Loiseau, G. Rigas, S. L. Brunton, Nonlinear stochastic modelling with langevin regression, Proceedings of the Royal Society A 477 (2021) 20210092.

[46] S. Zhang, G. Lin, Robust data-driven discovery of governing physical laws with error bars, Proceedings of the Royal Society A: Mathematical, Physical and Engineering Sciences 474 (2018) 20180305.

[47] T. Hastie, R. Tibshirani, J. H. Friedman, The elements of statistical learning: data mining, inference, and prediction, volume 2, Springer, 2009.

[48] R. Tibshirani, Regression shrinkage and selection via the lasso, Journal of the Royal Statistical Society Series B: Statistical Methodology 58 (1996) 267–288.

[49] A. Beck, Y. C. Eldar, Sparsity constrained nonlinear optimization: Optimality conditions and algorithms, SIAM Journal on Optimization 23 (2013) 1480–1509.

[50] Z. Yang, Z. Wang, H. Liu, Y. C. Eldar, T. Zhang, Sparse nonlinear regression: Parameter estimation under nonconvexity, in: International Conference on Machine Learning, PMLR, 2016, pp. 2472–2481.

[51] H. Zou, The adaptive lasso and its oracle properties, Journal of the American Statistical Association 101 (2006) 1418–1429.

[52] R. C. Aster, B. Borchers, C. H. Thurber, Parameter estimation and inverse problems, Elsevier, 2018.

[53] M. Raissi, P. Perdikaris, G. E. Karniadakis, Physics-informed neural networks: A deep learning framework for solving forward and inverse problems involving nonlinear partial differential equations, Journal of Computational Physics 378 (2019) 686–707.

[54] D. Oettinger, G. Haller, An autonomous dynamical system captures all LCSs in three-dimensional unsteady flows, Chaos: An Interdisciplinary Journal of Nonlinear Science 26 (2016).

[55] N. Boddupalli, T. Matchen, J. Moehlis, Symbolic regression via neural networks, Chaos: An Interdisciplinary Journal of Nonlinear Science 33 (2023).

[56] P. Gray, S. K. Scott, Chemical oscillations and instabilities: non-linear chemical kinetics, Oxford University Press, 1990.

[57] N. A. Daryakenari, M. De Florio, K. Shukla, G. E. Karniadakis, Ai-aristotle: A physics-informed framework for systems biology gray-box identification, PLOS Computational Biology 20 (2024) e1011916.

[58] P. Macheras, A. Iliadis, Modeling in biopharmaceutics, pharmacokinetics and pharmacodynamics: homogeneous and heterogeneous approaches, volume 30, Springer, 2016.

[59] S. H. Rudy, S. L. Brunton, J. L. Proctor, J. N. Kutz, Data-driven discovery of partial differential equations, Science Advances 3 (2017) e1602614.

[60] M. I. Asensio, L. Ferragut, On a wildland fire model with radiation, International Journal for Numerical Methods in Engineering 54 (2002) 137–157.

[61] A. D. Jagtap, K. Kawaguchi, G. E. Karniadakis, Adaptive activation functions accelerate convergence in deep and physics-informed neural networks, Journal of Computational Physics 404 (2020) 109136.